Effect of severe shot peening on ultra-high-cycle fatigue of a low-alloy steel

Libor Trško [a], Otakar Bokůvka [a], František Nový [a,c], Mario Guagliano [b,*]

[a] University of Žilina, Faculty of Mechanical Engineering, Department of Materials Engineering, Univerzitná 1, 010 26 Žilina, Slovak Republic
[b] Politecnico di Milano, Dipartimento di Meccanica, Via La Masa 1, 20156 Milan, Italy
[c] Research Centre of University of Žilina, Univerzitná 1, 010 26 Žilina, Slovak Republic

Article history:
Received 9 July 2013
Accepted 16 December 2013
Available online 21 December 2013

1. Introduction

Present development of new industrial machines requiring higher efficiency and cost savings must provide possibility of higher loading, higher operation speeds and high reliability together with reduced requirements for maintenance. For example, components of high speed train Shinkanzen in 10 years of operation have to withstand approximately $N = 10^9$ cycles and failure of a main component can have fatal consequences [1]. These facts increased requirements for fatigue life testing in so called ultra-high cycle region and to assess if the fatigue strength of a material could be really considered constant for more than 10 million cycles, conventional number of cycles used to determine the so called fatigue limit. Anyway, after the first tests performed by exceeding this endurance, it was obvious that fatigue failures can happen even for applied stress amplitudes lower than the fatigue limit, for a number of cycles much more than 10^7 and that the damage and failure process could be different form the usual ones.

However, to set a fatigue test program aimed at investigating the ultra-high cycle region requires the development of new testing devices to strongly increase the loading frequency. A symposium on this special topic was held in Paris in June 1998 where data obtained by high speed testing machines were presented by Stanzl-Tschegg [2] and Bathias [3] using ultrasonic fatigue testing machines capable of a frequency of 20 kHz, by Ritchie et al. [4] using a 1 kHz closed loop servo-hydraulic testing machine and by Davidson [4] using a 1.5 kHz magneto-strictive loading machine [1]. From that time many solutions were proposed but still the most commonly used machines for this kind of tests are based on concept of Manson from 1950 and uses frequencies close to 20 kHz. They represent a good balance between the strain rate, the determination of number of cycles to rupture and the duration of the fatigue test ($N = 10^{10}$ cycles are achieved in about 6 days). Other devices able to get higher loading frequencies are rarely used because they cause extremely high deformation rates and, since the test lasts for only few minutes, a remarkable error in the cycle counting is expected [5].

But the investigation of a material in the ultra high-cycle fatigue regime also raises other questions about the successful application of the methods commonly used to improve the fatigue behavior of metal alloys and structural/machine parts. In particular, it is well known that mechanical treatments can be successfully used to increase the fatigue limit, especially in the case of notched parts, but just a few investigations explore their application in the ultra high cycle fatigue.

* Corresponding author. Tel.: +39 0223998206; fax: +39 0223998263.
E-mail address: mario.guagliano@polimi.it (M. Guagliano).

Among these latter treatments, shot peening can be considered the most widely used, due to its flexibility, its relative low cost and due to the fact of reducing the environmental impact with respect of other treatments used with the same aim.

The positive effect of shot peening on the fatigue properties is generally related to its ability to introduce a compressive residual stress state in the surface layer of material and to the surface work hardening caused by the not uniform plastic deformation caused by the multiple impacts of the shot flow [6–10]. Many experimental evidences show that shot peening is more effective with steep gradient of the applied stress, while the effect is less evident when applied to smooth specimens subjected to axial fatigue, due to the fact that in this case the beneficial effect of the treatment on the surface can only shift the crack initiation point in the inner material (generally in correspondence of an internal material defect), without a relevant increment of the applied stress.

Recently, the possibility to use shot peening as a severe plastic deformation process was also investigated. Usual air blast devices with unusual severe process parameters (higher Almen intensity and coverage), characterized by high kinetic energy proved the ability to accumulate a great amount of plastic deformation causing grain refinement up to nanometer scale [11–16].

This treatment, called severe shot peening (SSP), resulted in improved properties of the treated layer of material: deeper residual stresses and surface work hardened layer, increased surface hardness. Some data [11] show also that SSP should be able also to increase the corrosion resistance, while it is known that conventional shot peening could decrease the corrosion properties [17]. Undesired side effect of SSP is an increment of the surface roughness.

However just a few data exists about the effect of SSP on steel fatigue behavior [11,12] and, even if they show a general positive effect of SSP on the fatigue strength (especially for notched specimens), it is true that the data are referred to just to few steel grades that do not allow to generalize the expected increment of the fatigue strength. Besides, the number of cycles chosen to define the run-out condition cannot guarantee that the improved behavior is maintained for more than 10 million cycles.

In this study steel 50CrMo4 used in automotive industry for car wheel hubs has been investigated. This component is cyclically loaded and subjected to fatigue; after years of operation may accumulate quite a number of fatigue cycles, greatly exceeding 10 million cycles, usually considered for conventional fatigue limit evaluation. Anyway, there are practically no available data about fatigue behavior in the ultra-high cycle region of this material.

Axial fatigue tests aimed at investigating the ultra-high cycle fatigue behavior were executed. Two series of smooth specimens were considered: mechanically polished and severely shot peened, being the aim to investigate the ability of this treatment to increase the fatigue strength of the material for very long expected endurance and to compare it with the non-treated state.

Roughness, microhardness, X-ray diffraction residual stress analysis and crystallite size measurement as well as scanning electron microscopy (SEM) observations were used for characterizing the severely deformed layer. Tension–compression high frequency fatigue tests were carried out to evaluate the effect of the applied treatment on fatigue life in the ultra-high cycle region. Fracture surface analysis was performed with aim to investigate the mechanism of fatigue crack initiation and propagation by using SEM. Results show an unexpected significant fatigue strength increase in the ultra-high cycle region after SSP surface treatment and are discussed in the light of compression residual stress profile and crystallite size.

2. Material characterization

Quenched and tempered steel 50CrMo4 was considered in this study. The nominal chemical composition is shown in Table 1. Test specimens were machined from a die forged car wheel hub. The die forging was done in temperature range 850–1050 °C. After forging, the flange was quenched from austenitization temperature of 860 °C (holding time 1 h) to mineral oil. Right after quenching, the steel was tempered on temperature 600 °C for 1 h and then it was left to cool on calm air. The heat treatment resulted in mechanical properties shown in Table 2.

Due the big diameter of the forged piece (⌀75.5) the critical cooling rate for quenching could not be obtained in the whole diameter of the piece and the microstructure was changing from the surface towards to the core. Specimens were machined in position according to Fig. 1a so the axis of the specimen was distant 12 mm from the surface. This avoided the influence of decarburization and the gauge length of specimen represented the same microstructure as would be present in the surface layers of machined wheel hub.

To obtain the microstructure of the material in the gauge length of the specimen where fatigue damage occurs, a longitudinal cut of a specimen with initiated crack was done; the result is shown in Fig. 2. The microstructure consists of sorbite, bainite and imperfectly transformed ferrite and pearlite.

2.1. Surface characterization

Machined specimens were divided into two groups, each with 11 PCS. The first group was grinded and polished with diamond metallography emulsion (this group is marked as NP – not peened). The second group was treated by severe shot peening with S170 medium (steel shots, ⌀ = 425 μm), Almen intensity 15.6 A and coverage 1000% (this group is marked as SSP – severely shot peened). Two rods were machined for residual stress measurement (Fig. 1b) and treated as mentioned above (one NP and one SSP). Areas subjected to surface treatment for all specimens are marked A in Fig. 1b and c.

In Fig. 3 the surface layer of NP and SSP specimen is shown. The surface layer of NP specimen (Fig. 3a) after mechanical polishing has no deformed surface layer and high quality surface with low roughness. On the contrary, the surface layer of SSP specimen (Fig. 3b) has a deep strongly deformed surface layer and also increase of surface roughness is obvious.

Due the character of quenched and tempered microstructure it is not appropriate to consider a grain size value which is mainly referred to optical microscopy analysis. In terms of X-ray diffraction the analysis is referred to crystallite size which is the size of coherently diffracting domains of crystals and grains may contain several of these domains. After plastic deformation of a single crystal several sub-crystals will be created and these can be considered as the crystallites. For more information about crystallite size measurement by XRD diffraction, the reader can refer to [18,19]. According to XRD measurement (X'Pert PRO diffractometer, Co radiation, diffraction angles from 45° to 130° (2θ), parallel plate collimator, crystallite size evaluated with TOPAS software according to all four diffraction lines {1 1 0, 2 0 0, 2 1 1, 2 2 0}), the crystallite size on the surface decreased from average value of 74 ± 3 nm for the NP specimen to 38 ± 4 nm for the SSP specimen. This layer with different appearance in secondary electron SEM analysis corresponds to so called "nano grained" or "ultra-fine grained" surface layer of material (Fig. 4). Plastic deformation was so intensive that part of the surface layer peeled off (Fig. 5) and also caused a remarkable increase of surface roughness compared to the NP specimens, as shown in Table 3.

2.2. Hardness measurement

Presence of compressive residual stress and surface hardened layer can be indirectly evaluated by microhardness measurement,

Table 1
Chemical composition of steel 50CrMo4 according DIN EN 10083-3 (wt.%).

C	Mn	Si (max.)	P (max.)	S (max.)	Cr	Mo	Fe
0.46–0.54	0.50–0.80	0.40	0.025	0.035	0.90–1.2	0.15–0.30	Balance

Table 2
Mechanical properties of steel 50CrMo4 after quenching and tempering.

UTS (MPa)	Proof stress (MPa)	A (%)	Z (%)
929	702	15.0	54.7

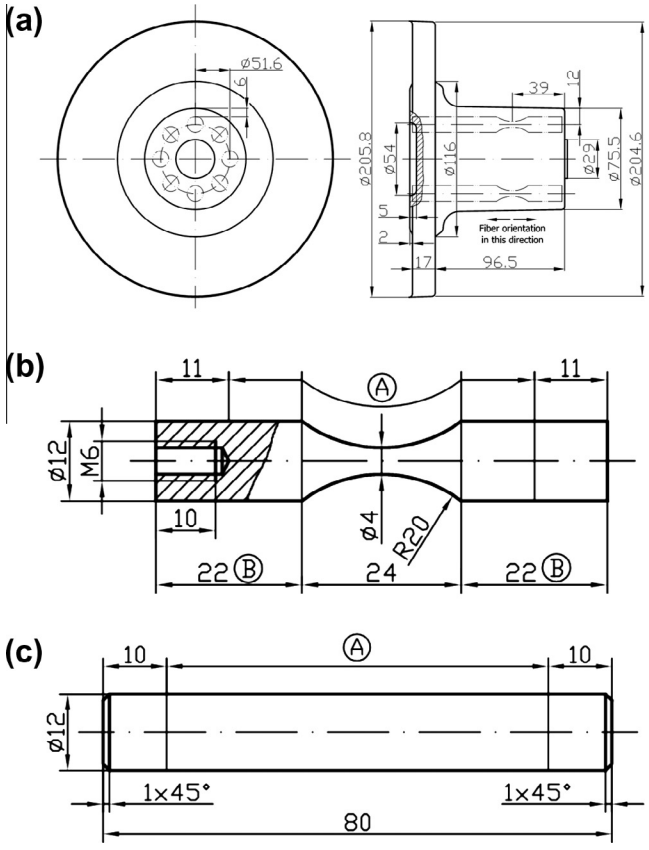

Fig. 1. Drawing of die forged wheel hub and position of machined specimens (a), geometry of specimens used for high frequency fatigue tests (b) and rods for residual stress measurement (c). All dimensions are given in mm.

because microhardness values are very sensitive to dislocation density which increases after plastic deformation. Microhardness measurement was done on a cross cut of ∅12 mm rod with load of 50 gf (HV0.05 according to standard [20]) in row from the surface to the core of the material with step of 0.05 mm. Three series of measurements were performed for each specimen. The first point of microhardness obtained at depth 0.025 mm was not measured in the same row as the rest of the values, because it might be affected by the other indentation and also there is an influence of free surface, so the first point does not fulfill the requirements of mentioned standard. Results of microhardness measurement are shown in Fig. 6. According to these results it can be considered, that after SSP application the microhardness in depth of 0.025 mm increased from about 280 HV0.05 to 370 HV0.05 and it is continuously decreasing on the same value as for NP specimen in depth of 0.15 mm. This can be considered as the first mark of the presence of work hardened layer induced by SSP and of the consequent introduction of a residual stress field.

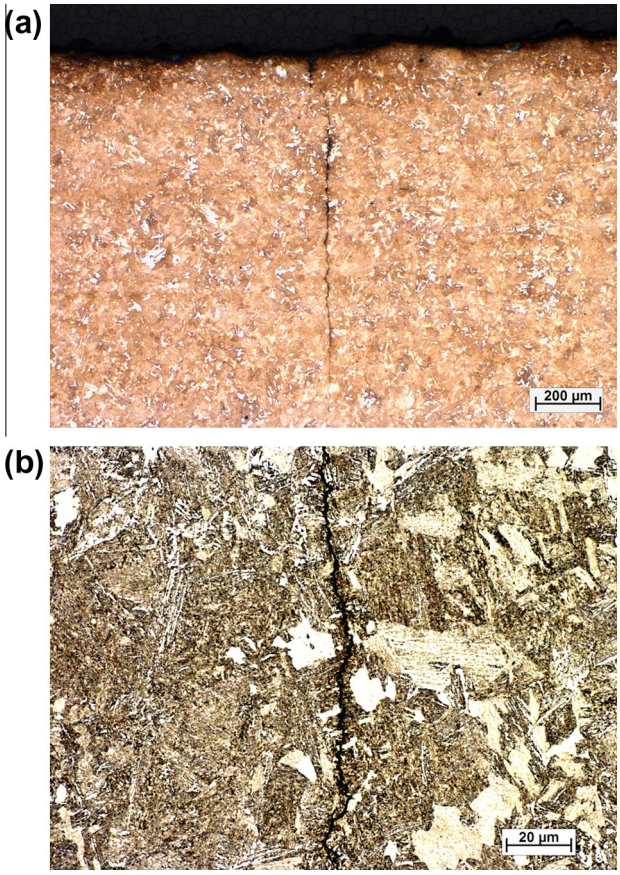

Fig. 2. Microstructure of the material in the central part of the tested specimen in the surrounding of the crack in macro view (a) and in detail (b).

2.3. Residual stress measurement

To obtain quantitative values of the residual stresses in the material X-ray diffraction (XRD) measurements were carried out by means of X-Stress 3000 StressTech device (Cr radiation Kα, irradiated area of 1 mm^2, sin^2 ψ method, diffraction angles (2θ) scanned at 11 different ψ angles ranging from −45° to 45°). Due the curvature of the fatigue specimen the measurements were executed in the 90° direction (Fig. 7c) while it was not possible to measure other stress components to determine the complete stress tensor and the principal stresses. This is the reason why the cylindrical rods (Fig. 1c) were used to obtain complete residual stress profile in three directions in both in NP and SSP states. The resulting residual stress profiles of these rods are shown in Fig. 7a and according to them it can be argued that both rods were subjected to an almost equi-biaxial compressive residual stress state. After machining a polishing (NP) the strengthened layer of material is very thin and the compressive residual stress disappears in 0.04 mm from the surface. On the contrary, the compression residual stress after SSP application has at this depth its maximum and then slightly decreases until depth of 0.3 mm, then it starts rapidly dropping and meets the value of NP material in the depth of 0.47 mm. During the residual stress measurement the FWHM parameter (Full Width at Half Maximum)

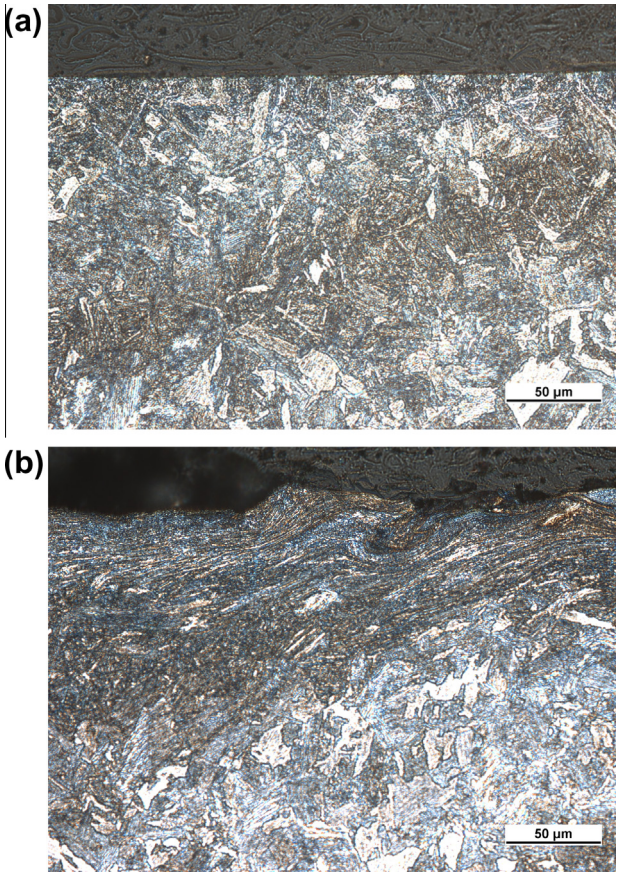

Fig. 3. Surface of NP (a) and SSP (b) specimen, longitudinal cut, etch. Nital.

was also obtained, which is defined as the width of the diffraction peak in half of its height and it is related both to residual microstrain in the material and to the grain size [21]. By summarizing it can be considered as a comparative index of the surface work hardening. According to FWHM profile (Fig. 7b) it can be noted the strong surface hardening after SSP and that the SSP trend meets the FWHM profile of NP rod at a depth of 0.4 mm.

Residual stress profiles of NP and SSP specimens were measured in the middle of the specimen, where the nominal diameter is 4 mm. As mentioned, good collimation of the X-ray was possible only in the angle 90°. When comparing the residual stress and FWHM profile for the SSP rod and SSP fatigue specimen (Fig. 8a), it is observed that the compression residual stresses are deeper in the rod than in the fatigue specimen (the values of residual stresses in the fatigue specimen starts dropping in depth of 0.2 mm under the surface), but that the values of the compression residual stress are higher in the fatigue specimen than in the rod. According to this it can be argued, that the deformation energy stored in the material by SSP application is approximately the same for both specimens, but the curvature of the fatigue specimen has an important influence on the compression residual stress distribution. In fact, the smaller the cylinder diameter, the larger the Hertzian contact stress as well as the compressive residual stress. Besides, the contact conditions realized with the assigned treatment parameters give a more severe plastic deformation on the surface of the fatigue specimen. At the same time, the small diameter causes a reduction of the compressed layer due to the fact that tensile stresses must contract the compressive ones to have a self-balanced stress field.

This behavior is not so obvious looking at the FWHM profile, but it can be observed that the surface work hardening is higher in the fatigue specimen than in the rod (Fig. 8b).

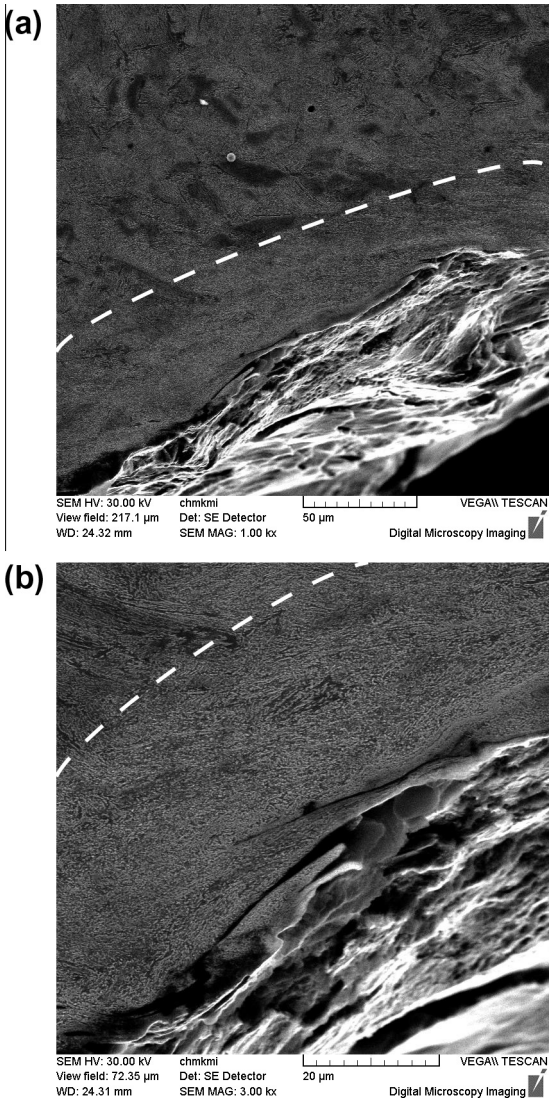

Fig. 4. Surface of a SSP specimen with nano (ultrafine) grain character (a) and with a higher magnification factor (b); white dashed line marks the approximate boundary between the nano-grained surface layer and the base material, longitudinal cut, etch. Nital.

The residual stresses were measured on the fatigue specimens also after the end of a run-out test. As expected, residual stresses partially relaxed during the test. In Fig. 9a the residual stress in-depth trend for a run-out specimen ($\sigma_a = 365$ MPa, $N = 1.55 \times 10^8$ cycles) is shown and compared with the one obtained before the test on SSP specimen. It is evident that after the test the residual stresses strongly decrease; more than 200 MPa are lost and the compression residual stress starts dropping in 0.1 mm under the surface. Even the FWHM trend shows a decrement after the test, even if the in-depth profile is more stable and the surface value is close to the un-cycled specimen (Fig. 9b).

3. Fatigue tests

High frequency tension – compression fatigue tests (stress ratio $R = -1$, frequency $f \approx 20$ kHz, temperature $T = 20 \pm 5$ °C) in high and ultra-high cycle region were carried out on high frequency experimental test device KAUP (complex acoustic fatigue toughness) of the Department of Materials Engineering, University of Žilina, Slovakia (Fig. 10). During the test, the specimen is cooled in water with anticorrosive inhibitor, used to provide full

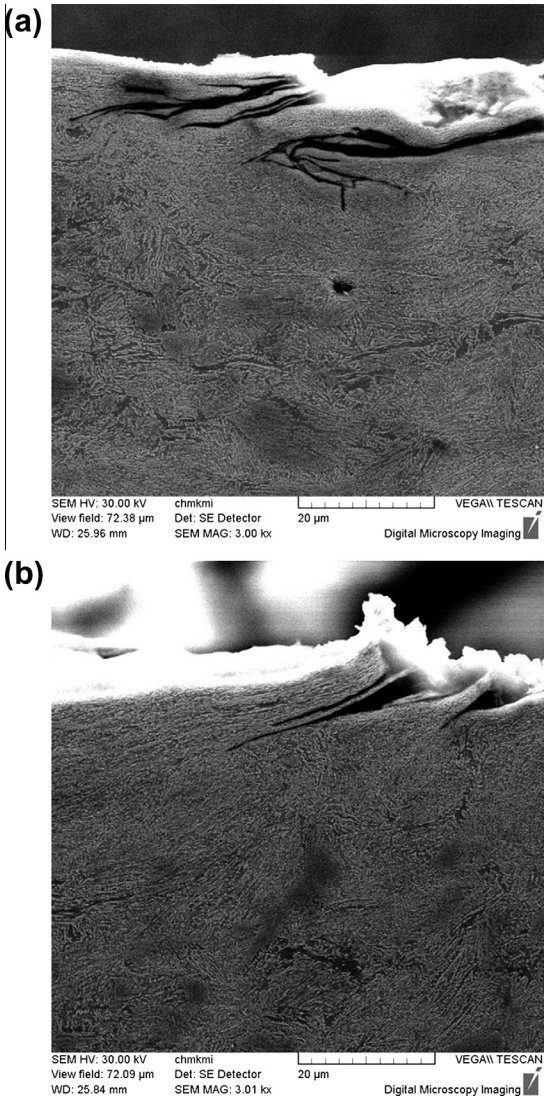

Fig. 5. Damage of the surface layers – material peeling off from the surface (a), sharp notch under the peeling off material layer (b), longitudinal cut, etch. Nital.

Table 3
Roughness parameters of used specimens.

	Ra (µm)	Rz (µm)
Not peened	0.4	2.6
Severe shot peened	5.4	27.9

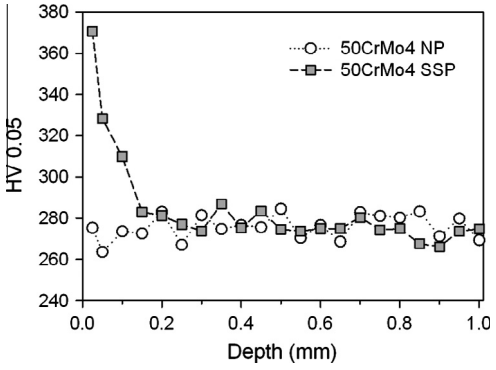

Fig. 6. In-depth microhardness trend.

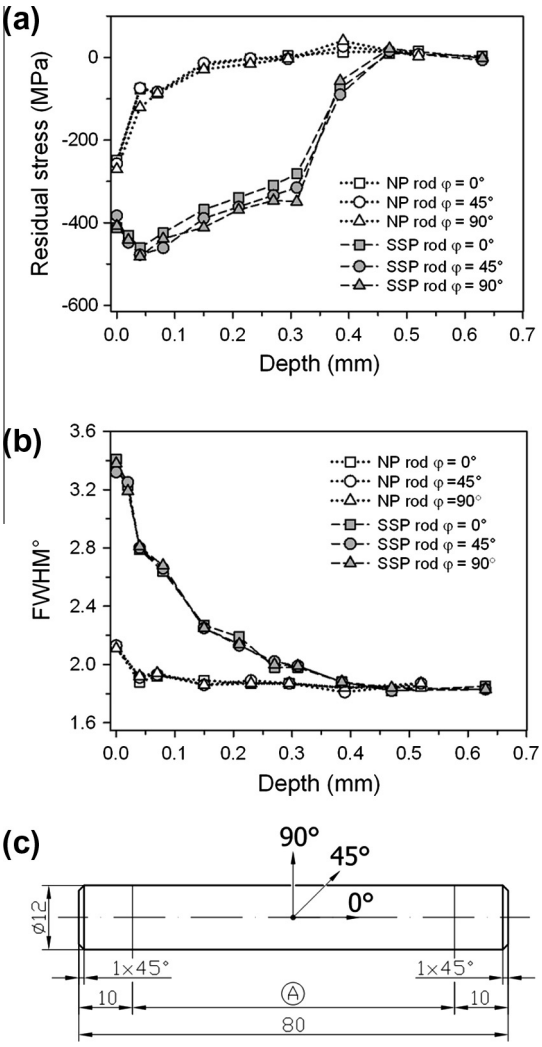

Fig. 7. In-depth residual stress profile (a) and FWHM profile (b) of rods, explanation of measuring angles (c).

short-time passivation of the steel surface [22]. The electric power from ultrasonic generator is transferred to mechanical vibration in the piezo-ceramic converter of the ultrasonic horn. This causes vibration of both ends of the specimen at resonance frequency. The power is increased until requested displacement amplitude is obtained (measured by displacement amplitude reader on the end of the specimen). The displacement amplitude is in linear correlation with electric current value on the input of the piezo-ceramic converter. A current probe measures this value. Due the heating of the specimen the resonance frequency slightly changes during the measurement (increase of the temperature causes decrease of the resonance frequency). This is compensated by computer program, which reads the value of input current from the current probe and automatically adjusts the frequency of ultrasonic generator. By this close loop system the power input in the ultrasonic horn is constant what keeps the stress amplitude of the specimen constant (the displacement amplitude can slightly change due the process of deformation strengthening or softening during the cyclic loading).

For fatigue tests specimens according Fig. 1a were used. Dimension marked B was adjusted separately for each specimen to accomplish the condition of Eq. (1):

$$f_{horn} = f_{horn+specimen} \quad (1)$$

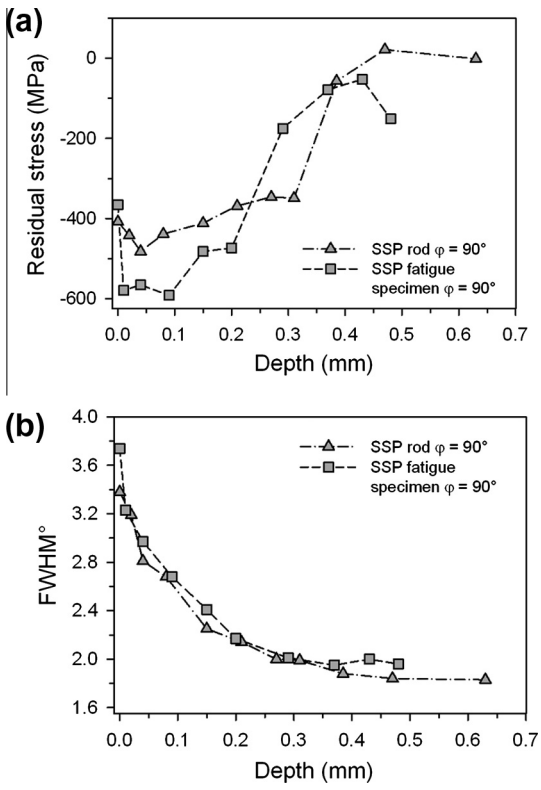

Fig. 8. Comparison of residual stress profile of rod and fatigue specimen (a) and FWHM profile (b).

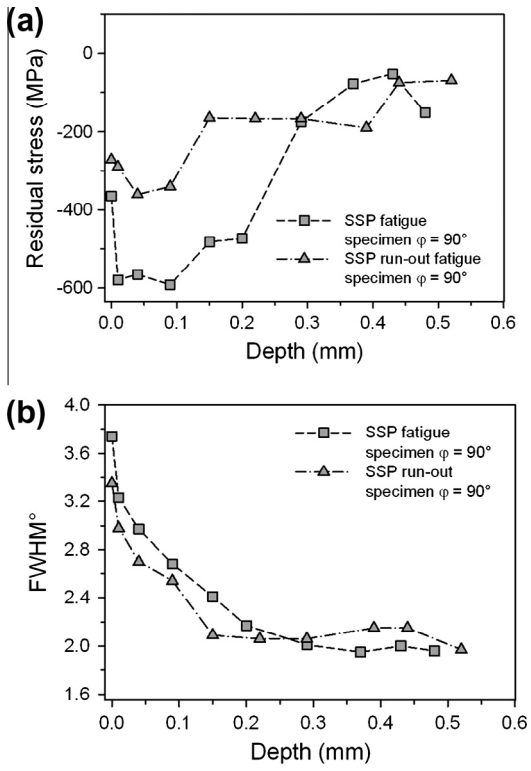

Fig. 9. Comparison of residual stress profile (a) and FWHM profile (b) before and after fatigue test.

where f_{horn} is the resonance frequency of ultrasonic horn by itself and $f_{horn+specimen}$ is the resonance frequency of the system horn with mounted specimen. The results of the fatigue tests, stress amplitude

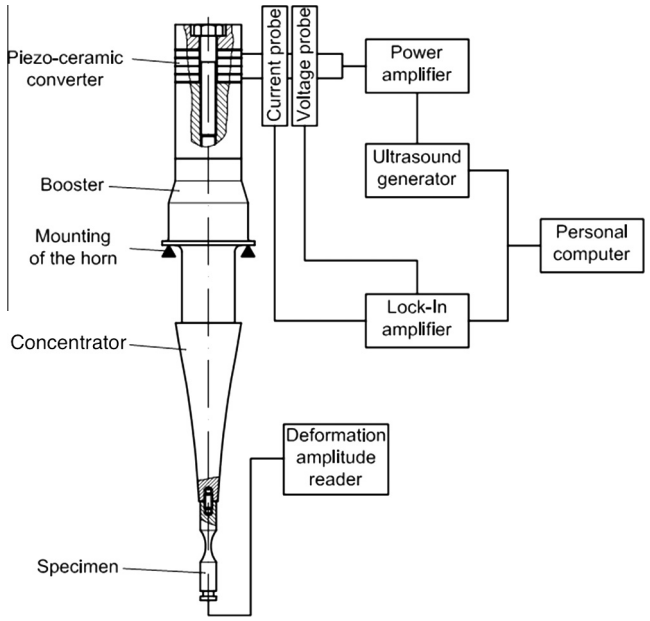

Fig. 10. KAUP device for ultrasonic fatigue tests at frequency $f \approx 20$ kHz.

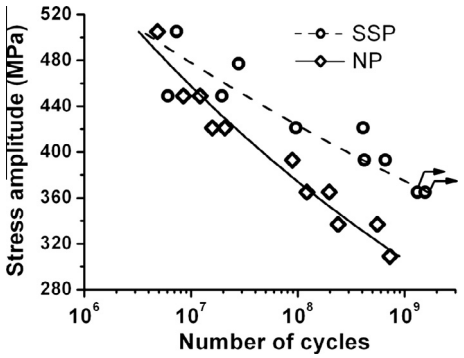

Fig. 11. Tension–compression fatigue curves of NP and SSP specimens ($R = -1$, $f \approx 20$ kHz, $T = 20 \pm 5$ °C).

vs. number of cycles to failure (or run-out), S–N curves are shown in Fig. 11. Results were approximated by the Basquin function (Eq. (2)) with use of least square method [23]:

$$\sigma_a = \sigma'_f \times (N_f)^b \tag{2}$$

where σ_a is the stress amplitude, σ'_f is the coefficient of fatigue toughness, N_f is the number of cycles to failure and b is the exponent of fatigue life curve. Coefficients of regression curves for both types of specimen are in Table 4.

According to the fatigue test results and regression curves it can be seen that fatigue strength of experimental material after SSP significantly increases in the ultra-high cycle region (for $N > 10^7$ cycles) and the fatigue strength improvement gets higher with the number of cycles (Table 5). The lowest tested stress amplitude applied on a NP specimen was $\sigma_a = 309$ MPa and the specimen withstood $N = 7.28 \times 10^8$ cycles before fracture. After SSP application, run-out at 1.55×10^9 cycles was determined at a stress amplitude $\sigma_a = 365$ MPa . On the contrary, in the high-cycle regime ($N < 10^7$ cycles) at about $N = 4 \times 10^6$ cycles the curves tend to converge. For $N < 4 \times 10^6$ it is possible to affirm that the fatigue strength will be lower for the SSP specimens than for the NP specimens. This is also obvious on the values of coefficient of fatigue toughness σ'_f, which is the stress value in which the regression

Table 4
Coefficients of the Basquin equation.

Surface treatment	σ'_f	b
NP	1869	−0.0873
SSP	1117	−0.0527

Table 5
Fatigue strength of not peened and severely shot peened specimens, $N = 10^7, 10^8, 10^9$.

	Fatigue strength for $N = 10^7$ (MPa)	Fatigue strength for $N = 10^8$ (MPa)	Fatigue strength for $N = 10^9$ (MPa)
Not peened	458	374	306
Severe shot peened	478	423	375
Increase	20	49	69

curve reaches the y-axis. The value σ'_f for NP series is equal to 1869 MPa, higher than the value of the SSP series, which is 1117 MPa. This material behavior after peening application was confirmed also in [24].

4. Fracture surface analysis

From the comparison of fracture surface of NP and SSP specimen it is obvious, that in both cases only one crack initiated and propagated through the cross section of the specimen (Fig. 12a and b). One crack initiation site is typical for ultrasonic high frequency fatigue testing, because crack initiation changes the toughness of the system and frequency must be continuously adjusted so the crack is able to propagate. For more information about specific fatigue testing using this equipment, reader can refer to [5]. A more accurate observation of the fracture surfaces allows to note that the fracture surface is covered by oxide film, which was created by the passivation effect of the coolant in which was the specimen submerged. This passivation film degrades the quality of fracture surface analysis, but even due this fact, the most important characteristics of the fracture still can be evaluated. An important aspect that can be observed is the place of fatigue crack initiation.

On NP specimen the fatigue crack initiated on the free surface, probably in correspondence of a micro notch due to surface roughness after polishing (Fig. 13a). In Fig. 13b the crack initiation point of a SSP specimen is shown; it is noted that even in this case the crack initiation point is on the free surface, this is unusual for surface treated smooth specimens under axial load, since it is assumed that after surface strengthening the fatigue crack initiation is shifted toward the subsurface layers and a fish-eye can be created, but the microcracks created by peeling off layers of material due the severe plastic deformation created a stress concentration point where the fatigue crack initiated (Fig. 13b).

Due the severe shot peening affects only surface and subsurface layers of material, the aspect of fatigue crack propagation was the same in both series of specimens, trans-crystalline fatigue fracture (Fig. 14a and b). Besides the trans-crystalline fatigue mechanism, on the fracture surface some facets of inter-crystalline fatigue fracture are also occasionally present (Fig. 15a and 15b). These facets were created on weaken grain boundaries due micro segregation of elements during the steel manufacturing process. Striations perpendicular to the direction of fatigue crack propagation were present only in few places of fracture surface and they cannot be taken as a characteristic sign of fatigue fracture of this material (Fig. 16a and b).

Final fracture had the same character in all NP and SSP specimens and is trans-crystalline ductile fracture with dimple morphology (Fig. 17a). The size of the dimples depended on the

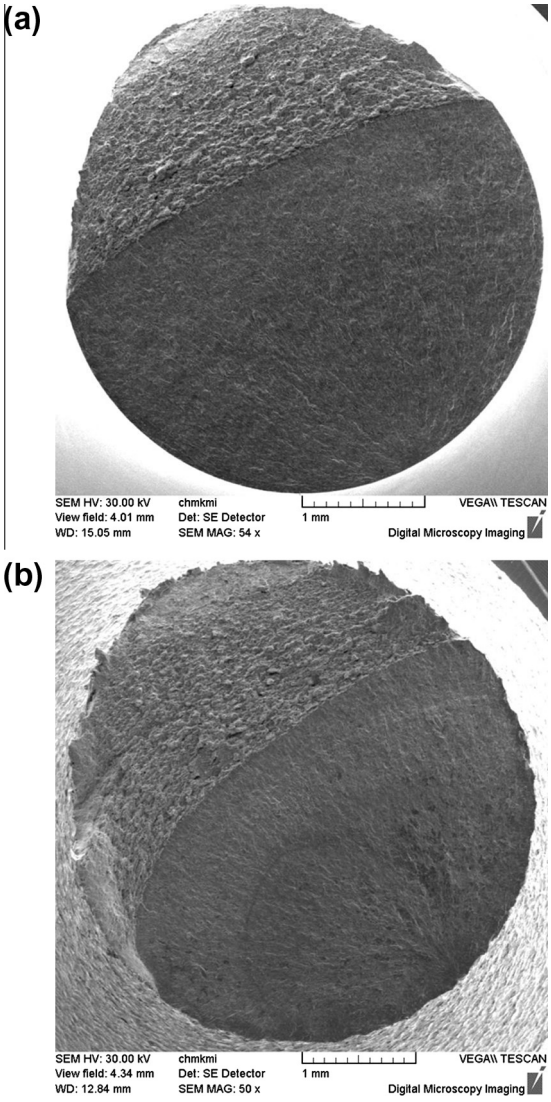

Fig. 12. SEM images of the fracture surface of fatigue specimens (a) NP specimen, $\sigma_a = 505$ MPa, $N_f = 4.87 \times 10^6$ cycles; (b) SSP specimen, $\sigma_a = 449$ MPa, $N_f = 1.95 \times 10^7$ cycles.

microstructure and the smallest dimples were created in places, where sorbite microstructure was present. In the final fracture were present small areas fractured by trans-crystalline cleavage mechanism with river morphology (Fig. 17b).

5. Discussion

The fatigue test results show that severe shot peening is able to improve the fatigue strength and life of the steel 50CrMo4 in the ultra high cycle fatigue regime. This fact can appear unexpected, since it is well known that shot peening, even if performed with unusual severe parameters, is able to affect the behaviour of the materials just in the sub-surface layer of material. That is to say that since axial fatigue tests were performed on smooth specimens, with a uniform distribution of the stress along the specimen section, the expected effect of shot peening was just to shift the crack initiation point, from the surface to an internal location (generally a non metallic inclusion).

This is true in the high-cycle fatigue regime and expected in the ultra high cycle regime, where, even without any surface

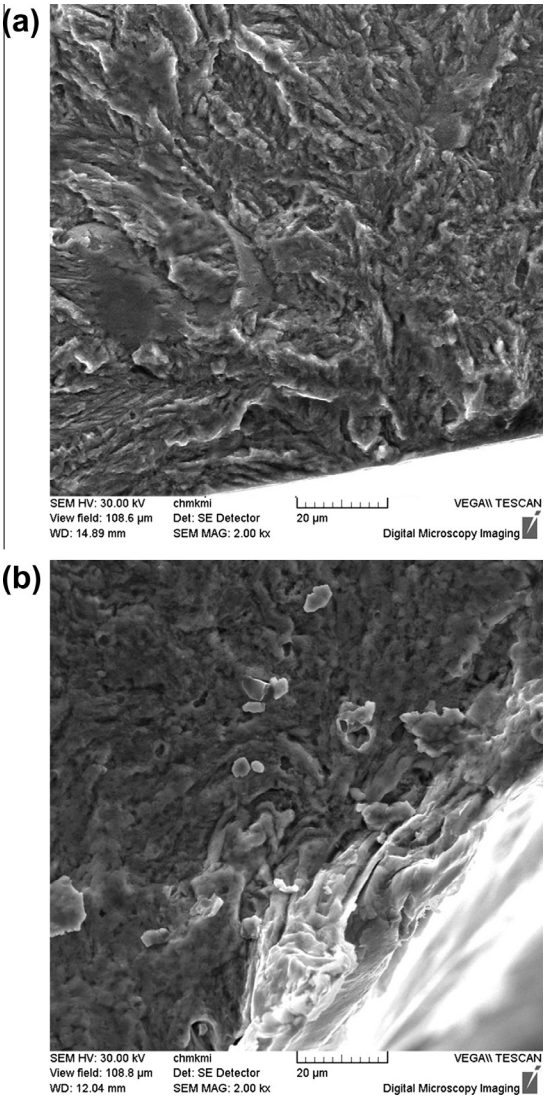

Fig. 13. Detail of fatigue crack initiation (a) NP specimen, $\sigma_a = 505$ MPa, $N_f = 4.87 \times 10^6$ cycles; (b) SSP specimen, $\sigma_a = 449$ MPa, $N_f = 1.95 \times 10^7$ cycles.

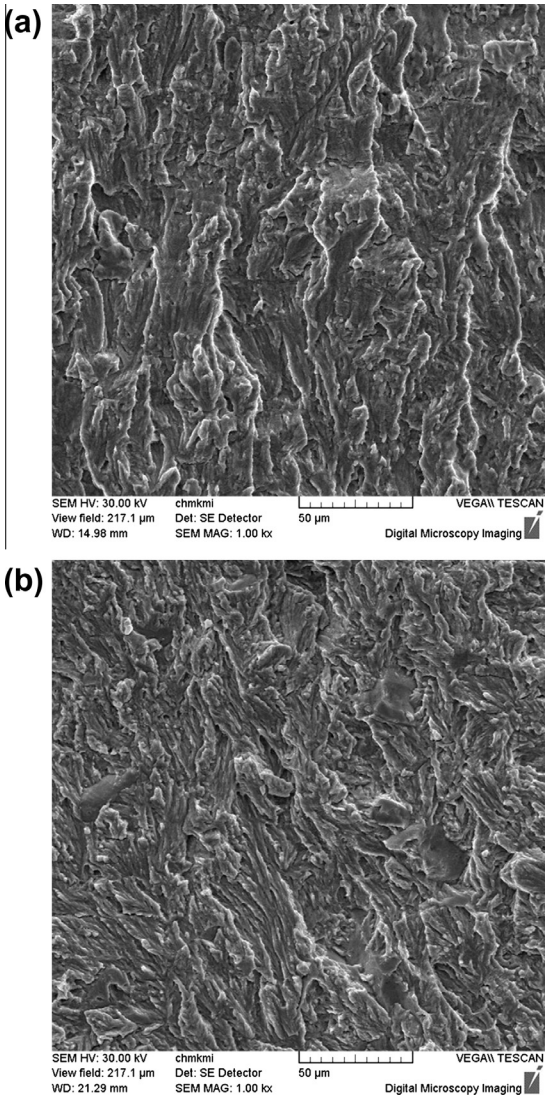

Fig. 14. Fatigue crack propagation (a) NP specimen, $\sigma_a = 505$ MPa, $N_f = 4.87 \times 10^6$ cycles; (b) SSP specimen, $\sigma_a = 393$ MPa, $N_f = 4.20 \times 10^8$ cycles.

treatment, it is common that the fatigue crack does not start from the surface [1,25–27].

But the experimental tests show that in this case the fatigue cracks always start from the surface; it can be argued that the material does not present anomalous defects (that were not observed in the fractographic analysis) or the presence of high tensile residual stresses under the peened layer [28,29]. The crack initiation points for SSP specimens were the extremely sharp notches induced by the modified roughness with peeling due the severe plastic deformation (Fig. 5b).

Experimental evidence shows also that severe shot peening is able to improve the fatigue strength and that the improvement increases with the number of cycles of interest. Indeed the improvement of the fatigue strength is as usual (about 5%) if $N = 10^7$ is considered for run-out specimens and the effect tend to decrease by decreasing the number of cycles. But if longer durations are considered the effect induced by severe shot peening becomes more and more marked and the increase is about 23% if $N = 10^9$ is considered. These results can be interpreted by considering all modifications induced by severe shot peening in the surface layer of material.

As concern the residual stresses introduced by shot peening it is clear that, even for the lowest stress amplitude they partially relax: about one half of the maximum compressive stress and of the compressed layer of material is lost during the test (Fig. 8). On this experimental basis and bearing in mind that residual stress relaxation is supposed to happen in the first thousand of cycles of the test, it can be argued that the residual stresses are not the most important effect in the modified behaviour of the shot peened specimens.

The second effect of severe shot peening, the modification of the roughness, is really relevant: the roughness parameters show a marked increment after shot peening (about ten time higher than in the NP specimens): since roughness affects negatively the fatigue strength, this could be considered a factor able to shift the fatigue crack initiation point from an internal defect to the free surface. But, since the fatigue strength improved after SSP, it seems a contradiction to affirm that roughness is able to shift the crack initiation point to the surface while improving the fatigue strength. And, indeed, even for the not peened specimens failure started from the surface. The conclusion is that roughness cannot be considered as a leading factor for interpreting the results of the experimental tests.

If the experimental XRD measurements and the SEM observations are considered, it is clear that severe shot peening induces strong changes of the material structure by refining the grain size

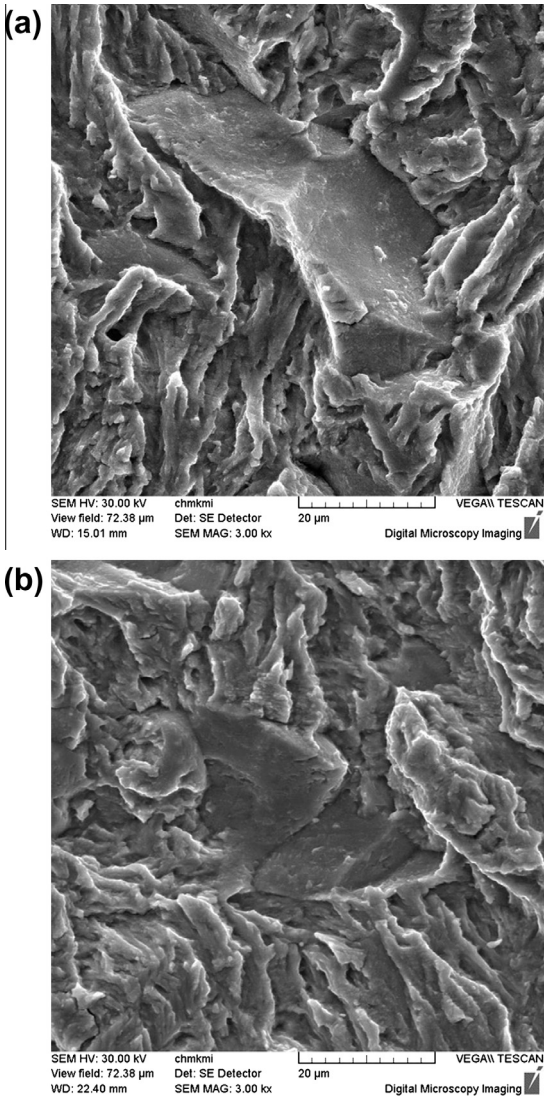

Fig. 15. Facets of intercrystalline fracture (a) NP specimen, $\sigma_a = 505$ MPa, $N_f = 4.87 \times 10^6$ cycles; (b) SSP specimen, $\sigma_a = 337$ MPa, $N_f = 5.55 \times 10^8$ cycles.

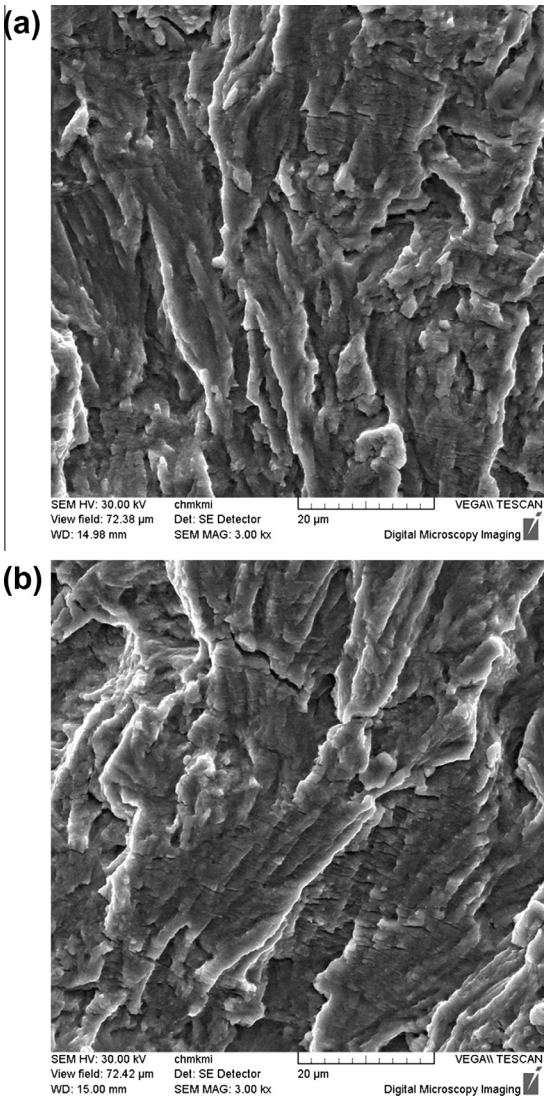

Fig. 16. Localities of fracture surface with fine striations (a) NP specimen, $\sigma_a = 505$ MPa, $N_f = 4.87 \times 10^6$ cycles; (b) SSP specimen, $\sigma_a = 449$ MPa, $N_f = 1.95 \times 10^7$ cycles.

up to less than 100 nm. And the FWHM trend shows a substantial stability of the material structure during the fatigue tests, without any significant changing.

The experiments show also that the thickness of the material layer affected by SSP is about 20 μm in terms of grain refinement to the nanoscale and about 0.2 mm in terms of work-hardened layer.

This means that the layer of material where fatigue damage takes place is modified by SSP. This is supposed to be the main factor for the improved fatigue behaviour of the SSP specimens in the ultra-high-cycle fatigue regime.

But, something remains to be completely explained as regards the reduced effect of severe shot peening in the high-cycle fatigue regime ($N \leqslant 10^7$): why the effect of the microstructural changing is not so remarkable in the high-cycle fatigue regime? The experimental results can be explained only by considering that a different damage mechanism takes place in this endurance range and by taking into account that the main effects caused by severe shot peening (residual stresses, grain refinement with surface work hardening and surface roughness) play a different role with respect of the fatigue damage in the ultra-high cycle regime.

Indeed, the high value of surface roughness and the sharp notches created by peeling the surface cause a pronounced local notch effect, that is a preferential site for crack initiation. Once the crack initiates, it finds a favourable media to propagate in the grain refined layer, characterized by reduced ductility [30]. If the test is performed in the high-cycle regime, the relaxation of the residual stresses, together with the uniform distribution of the applied stresses along the minimum section makes the crack, once initiated, able to propagate.

If the test is performed in the ultra-high cycle fatigue regime, the applied stress amplitude decreases and, notwithstanding the high surface roughness, crack propagation does not initiate. In this case it is possible to take full advantage of the grain refinement, which is able to increase the fatigue crack initiation stress. In fact, a very positive influence of nano-grained surface layer on fatigue properties of various materials obtained not only by severe shot peening, but also with other severe plastic deformation techniques, as ultrasonic nanocrystal surface modification, was confirmed in [31–33]. Besides, in this regime the value of the residual stresses, even if partially relaxed, is more relevant with respect of the applied stress and can contribute even to avoid crack propagation in its early stage.

By summarizing, the better behavior of the SSP specimens can be mainly ascribed to the nanocrystallized structure of the surface

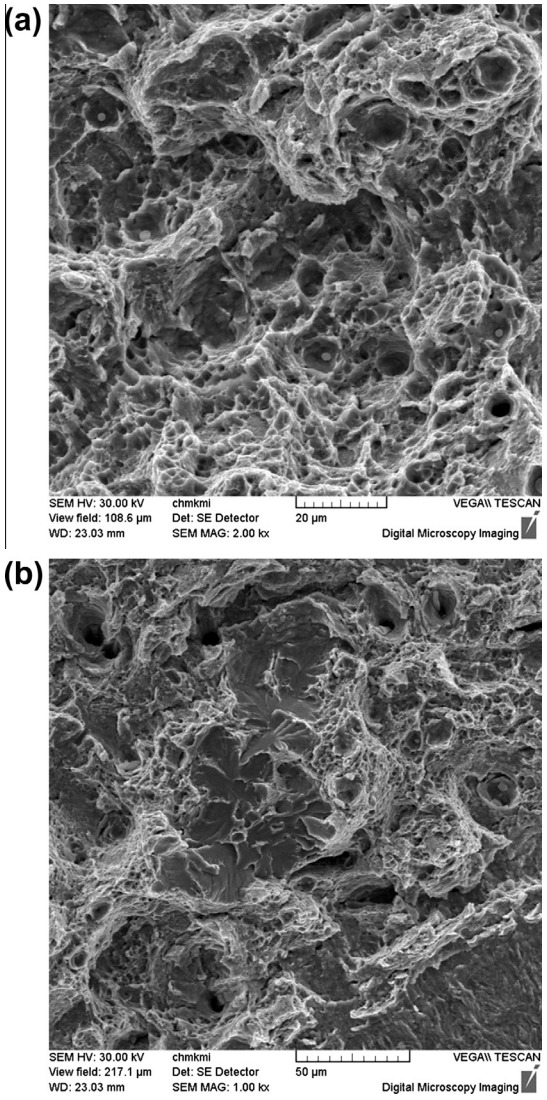

Fig. 17. Final fracture of SSP specimen, $\sigma_a = 477$ MPa, $N_f = 2.80 \times 10^7$ cycles: (a) trans-crystalline fracture with dimple morphology; (b) areas of trans-crystalline cleavage with river morphology.

layer of material, able to increase the stress to be applied for crack initiation; the role of the residual stresses is more remarkable in the UHCF regime, where the applied stress is lower than in the HCF and LCF fatigue region.

Due to these considerations, in the case of UHCF it is important the quality control of the material. It means that sharp non metallic inclusions should be avoided, since in this case the advantage got from the application of SSP could be vanished by crack initiation at an internal defect. This interpretation agrees with other papers (i.e. [12,34–36]) where smooth steel specimens subjected to bending fatigue show a limited benefit of SSP application in the high-cycle regime while notched specimens, due to the more pronounced gradient of the applied stress should, emphasize the role of SSP both in terms of microstructure and of residual stress retention.

6. Conclusions

50CrMo4 steel smooth specimens have been fatigue tested in the ultra high cycle regime. Before the tests, a set of specimens was severely shot peened (shot peened with unconventional and severe intensity and coverage). In the light of the results the following conclusions can be drawn:

- Severe shot peening is able to induce grain refinements up to less than 100 nm, thus producing a nanostructured surface layer of material.
- A compressive residual stress field in the surface layer together with high surface hardness is also observed after the treatment.
- The residual stresses generated by shot peening are partially lost during the fatigue tests: the maximum compressive stress and the depth of the compressive stress field are reduced to almost one half of the initial value. The microstructure and the related surface work hardening show a substantial stability after the tests.
- The results of the fatigue tests show an appreciable positive effect of SSP, especially in the ultra high cycle fatigue regime (up to 10^9 cycles): in this case the improvement due to SSP is about 23% while in the high cycle fatigue (10^7) the improvement is less evident.
- The results were interpreted in the light of the effect of the residual stresses, roughness and modified microstructure caused by SSP: a primary role of the structure modification is underlined while the effect of residual stresses is expected to be more relevant in the ultra high cycle regime. Since in this latter case fatigue cracks are not unusual to initiate from an internal inclusion, it is important to carefully check the impurities of the material to get the maximum advantage by the application of SSP.
- On the basis of the discussion of the results even better results are expected both in the ultra high cycle fatigue and in high cycle fatigue if notched specimens are considered, where the gradient of the applied stress should emphasize the role of the treated.

Acknowledgements

The research was supported by European regional development fund and Slovak state budget by the project "Research Centre of University of Žilina", ITMS 26220220183 and the Scientific Grant Agency of the Ministry of Education, Science and Sports of the Slovak Republic and Slovak Academy of Sciences, Grant No.: 1/0743/12. The authors thank Michele Bandini, Ph.D., and Peenservice srl for performing the shot peening treatments and for the valuable support in the development of the research.

References

[1] Murakami Y. Metal fatigue: effects of small defects and nonmetallic inclusions. 1st ed. Oxford: Elsevier; 2002.
[2] Stanzl-Tschegg SE. Fracture mechanisms and fracture mechanics at ultrasonic frequencies. Fatigue Fract Eng Mater Struct 1999;22:567–79.
[3] Bathias C. There is no infinite fatigue life in metallic materials. Fatigue Fract Eng Mater Struct 1999;22:559–65.
[4] Ritchie RO, Davidson DL, Boyce BL, Campbell JP, Roder O. High-cycle fatigue of Ti–6A1–4V. Fatigue Fract Eng Mater Struct 1999;22:621–31.
[5] Bokůvka O, Nicoletto G, Kunz L, Palček P, Chalupová M. Low and high frequency fatigue testing. 1st ed. Žilina: EDIS; 2000.
[6] Fernandez Pariente I, Guagliano M. Contact fatigue damage analysis of shot peened gears by means of X-ray measurements. Eng Fail Anal 1999;16:964–71.
[7] Yu-Kui G. Influence of shot peening on tension–tension fatigue properties in Ti–10V–2Fe–3Al titanium alloy. Chin J Nonferr Metals 2004;1:60–3.
[8] Zhang P, Lindemann J, Leyens L. Shot peening on the high-strength magnesium alloy AZ80 – effect of peening media. J Mater Proc Technol 2010;210:445–50.
[9] Luong H, Hill MR. The effects of laser peening and shot peening on high cycle fatigue in 7050–T7451 aluminum alloy. Mater Sci Eng 2010;527:699–707.
[10] Miková K, Guagliano M, Bokůvka O, Trško L, Nový F. The role of shot peening in increasing of X70 steel fatigue properties. Commun Sci Lett Univ Žilina 2012;14:94–8.

[11] Bagheri S, Guagliano M. Review of shot peening processes to obtain nanocrystalline surfaces in metal alloys. J Surf Eng 2009;25:3–14.
[12] Bagherifard S, Guagliano M. Fatigue behaviour of a low-alloy steel with a nanostructured surface obtained by severe shot peening. Eng Fract Mech 2012;81:56–68.
[13] Wen AL, Ren RM, Wang S, Yang JY. Effect of surface nanocrystallization method on fatigue strength of TA2. Mater Sci Forum 2009;620:545–9.
[14] Roland T, Retraint D, Lu K, Lu J. Fatigue life improvement through surface nanostructuring of stainless steel by means of surface mechanical attrition treatment. Scr Mater 2006;54:1949–54.
[15] Li D, Chen HN, Xu H. The effect of nanostructured surface layer on the fatigue behaviors of carbon steel. Appl Surf Sci 2009;255:3811–6.
[16] Shaw LL, Tian JW, Ortiz AL, Dai K, Villegas JC, Liaw PK, et al. A direct comparison in the fatigue resistance enhanced by surface severe plastic deformation and shot peening in a C-2000 superalloy. Mater Sci Eng 2010;527:986–94.
[17] Hadzima B, Bukovina M, Doležal P. Shot peening influence on corrosion resistance of AE21 magnesium alloy 2010. Mater Eng 2010;17:14–9.
[18] Vajpai SK, Dube RK, Sharma M. Studies on the mechanism of the structural evolution in Cu–Al–Ni elemental powder mixture during high energy ball milling. J Mater Sci 2009;44:4334–41.
[19] Fitzpatrick ME, Fry AT, Holdway P, Kandil FA, Shackleton J, Suominen L. Determination of residual stresses by X-ray diffraction. Meas Good Pract Guide 2005;52:1–68.
[20] EN ISO 6507–1: 2005 Vickers Hardness Test.
[21] Farrahi GH, Lebrun JL. Surface hardness measurement and microstructural characterisation of steel by X-ray diffraction profile analysis. J Eng 1995;8(159):67.
[22] Hadzima B, Suchý P. Short-time passivation of WNr.1.7139 steel surface. Mater Eng 2007;14:31–4.
[23] Kohout J, Věchet S. A new function for fatigue curves characterization and its multiple merits. Int J Fatigue 2001;23:175–83.
[24] Škorík V, Nový F, Doležal P, Hadzima B, Horynová M. Impact analysis of shot peening of aluminium alloy AW 6082 on the fatigue properties. In: Yucomat: proceedings of the 13th annual conference 2011, September 5–9, Herceg Novi, Montenegro, 2011. p. 112.
[25] Wang QY, Bathias C, Kawagoishi N, Chen Q. Effect of inclusion on subsurface crack initiation and gigacycle fatigue strength. Int J Fatigue 2002;24:1269–74.
[26] Shiozawa K, Morii Y, Nishino S, Lu L. Subsurface crack initiation and propagation mechanism in high-strength steel in a very high cycle fatigue regime. Int J Fatigue 2006;28:1521–32.
[27] Huang Z, Wagner D, Bathias C, Paris PC. Subsurface crack initiation and propagation mechanisms in gigacycle fatigue. Acta Mater 2010;58:6046–54.
[28] Mylonas GI, Labeas G. Numerical modelling of shot peening process and corresponding products: Residual stress, surface roughness and cold work prediction. Surf Coat Technol 2011;205:4480–94.
[29] Hong T, Ooi JY, Shaw B. A numerical simulation to relate the shot peening parameters to the induced residual stresses. Eng Fail Anal 2008;15:1097–110.
[30] Cavaliere P. Fatigue properties and crack behavior of ultra-fine and nanocrystalline pure metals. Int J Fatigue 2009;31:1476–89.
[31] Tian R, Wang Q, Liu Y, Pyoun YS. Effect of ultrasonic nanocrystal surface modification on ultra-long life fatigue properties of Ti-alloys. In: Berger C, Christ HJ, editors. Fifth international conference on very high cycle fatigue, DVM-Berlin, Germany, June 28–30, 2011. p. 411–8.
[32] Suh CM, Baek UB, Pyun YS, Cho IH. Torsion fatigue characteristics of torsion bar after ultrasonic-nanocrystal surface modification. In: Berger C, Christ HJ, editors. Fifth international conference on very high cycle fatigue, DVM-Berlin, Germany, June 28–30, 2011. p. 399–404.
[33] Pyun YS, CM Suh, Cho IH, Jung DH. VHCF characteristic of AISI 1045 and 4137, 52100 and H13 steel by ultrasonic nanocrystal surface modification. In: Berger C, Christ HJ, editors. Fifth international conference on very high cycle fatigue, DVM-Berlin, Germany, June 28–30, 2011. p. 393–98.
[34] Bagherifard S, Fernandez-Pariente I, Ghelichi R, Guagliano M. Fatigue behavior of notched steel specimens with nanocrystallized surface obtained by severe shot peening. Mater Design 2013;45:497–503.
[35] Soady KA, Mellor BG, Shackleton J, Morris A, Reed PAS. The effect of shot peening on notched low cycle fatigue. Mater Sci Eng 2011;8528:79.
[36] Baohua N, Zheng Z, Zihua Z, Qunpeng. Very high cycle fatigue behavior of shot-peened 3Cr13 high strength spring steel. Mater Design 2013;50:503–8.